

Provided for non-commercial research and education use.
Not for reproduction, distribution or commercial use.



(This is a sample cover image for this issue. The actual cover is not yet available at this time.)

This article appeared in a journal published by Elsevier. The attached copy is furnished to the author for internal non-commercial research and education use, including for instruction at the authors institution and sharing with colleagues.

Other uses, including reproduction and distribution, or selling or licensing copies, or posting to personal, institutional or third party websites are prohibited.

In most cases authors are permitted to post their version of the article (e.g. in Word or Tex form) to their personal website or institutional repository. Authors requiring further information regarding Elsevier's archiving and manuscript policies are encouraged to visit:

<http://www.elsevier.com/copyright>



Amorphous interlayers between crystalline grains in ferromagnetic ZnO films

B.B. Straumal^{a,b,c,*}, S.G. Protasova^{a,b}, A.A. Mazilkin^{a,b}, B. Baretzky^c, A.A. Myatiev^d, P.B. Straumal^e, Th. Tietze^b, G. Schütz^b, E. Goering^b

^a Institute of Solid State Physics, Russian Academy of Sciences, Chernogolovka, 142432, Russia

^b Max-Planck-Institut für Intelligente Systeme (former MPI for Metals Research), Heisenbergstrasse 3, 70569 Stuttgart, Germany

^c Karlsruher Institut für Technologie, Institut für Nanotechnologie, Hermann-von-Helmholtz-Platz 1, 76344 Eggenstein-Leopoldshafen, Germany

^d National University of Science and Technology "Moscow Institute of Steel and Alloys – MISiS", Leninsky prospect 4, 119991 Moscow, Russia

^e A.A. Baikov Institute of Metallurgy and Materials Science, RAS, Leninsky prosp. 49, 117991 Moscow, Russia

ARTICLE INFO

Article history:

Received 6 November 2011

Accepted 7 November 2011

Available online 26 November 2011

Keywords:

Nanocrystalline materials

Amorphous materials

Grain boundaries

Magnetic materials

Thin films

ABSTRACT

The nanograined thin films of undoped ZnO were synthesized by the wet chemistry method. Films consist of the equiaxial nanograins, and possess ferromagnetic properties. Structural investigations by the XRD and HREM reveal that the crystalline wurtzite grains do not contact each other and are completely surrounded by a layer of amorphous phase. It forms a kind of continuous foam-like network, where the amorphous intergranular phase amount could be increased by the synthesis parameters. Simultaneously, the saturation magnetization increases as well.

© 2011 Elsevier B.V. All rights reserved.

1. Introduction

Transparent semiconducting ZnO would be a very attractive material for future spintronics applications, if it simultaneously possesses ferromagnetic (FM) properties [1–3]. Based on the *p*–*d* Zener-like model Th. Dietl et al. theoretically predicted that ZnO doped by the “magnetic” atoms like Mn, Co or Fe can become ferromagnetic at room temperature (RT) and above [4]. Summarizing 10 years effort of the investigations of diluted magnetic semiconductors and oxides, Th. Dietl underlined that the data on pure and doped ZnO remain quite contradictory [5]. Obviously, the bulk ZnO with uniformly distributed Mn atoms (or other “magnetic” dopants) is not ferromagnetic [5]. In order to elucidate the dependence of RT ferromagnetism on the microstructure in ZnO, we have recently analyzed a large series of experimental publications with respect to the present specific grain boundary (GB) area, i.e. the ratio of GB area to grain volume s_{GB} [6]. FM only appears, if s_{GB} exceeds a certain threshold value s_{th} . If the density of GB network is high enough, ZnO becomes ferromagnetic even without dopants [7,8]. Thus $s_{th} = (2 \pm 4) \times 10^5 \text{ m}^2/\text{m}^3$ for the Mn-doped ZnO and $s_{th} = (7 \pm 3) \times 10^7 \text{ m}^2/\text{m}^3$ for pure ZnO [6]. We observed recently that the crystalline wurtzite grains in FM Mn-doped ZnO are separated by amorphous layers [9,10]. The thickness of these layers increases with Mn contents [9,10]. The main goal of this work is to investigate the structure of grain boundaries and/or

that of intergranular layers in pure nanograined ZnO films and to search for structural reasons of their FM behavior.

2. Experimental

ZnO thin films consisting of dense equiaxial nanograins were produced by using the novel method of liquid ceramics [11]. Zinc (II) butanoate diluted in the organic solvent with zinc concentrations between 1 and 4 kg/m³ was used as a precursor. The butanoate precursor was deposited on (102) oriented sapphire single crystals. Drying at 100 °C in air (about 30 min) was followed by thermal pyrolysis in an electrical furnace in argon (1) at 650 °C, 0.5 h and (2) at 550 °C, 24 h. A similar method was recently proposed for zinc oleates [12]. The films were transparent and reveal sometimes a very slight greenish furnish. The thickness of the films was (1) 690 nm and (2) 370 nm, respectively. The film thickness was determined by means of electron-probe microanalysis (EPMA) and edge-on transmission electron microscopy (TEM). The presence of other magnetic impurities as Fe, Co, Mn and Ni was measured by atomic absorption spectroscopy in a Perkin-Elmer spectrometer and by electron-probe microanalysis (EPMA) and remained below 0.001 at.%. EPMA investigations were carried out in a Tescan Vega TS5130 MM microscope equipped by the LINK energy-dispersive spectrometer produced by Oxford Instruments. TEM investigations were carried out on a Jeol JEM-4000FX microscope at an accelerating voltage of 400 kV. The TEM samples were prepared by FIB technique. X-ray diffraction (XRD) data were obtained on a Siemens diffractometer (Co K_α radiation).

* Corresponding author at: Institute of Solid State Physics, Russian Academy of Sciences, Chernogolovka, 142432, Russia. Tel./fax: +7 499 2382326.

E-mail address: straumal@issp.ac.ru (B.B. Straumal).

3. Results and discussion

Fig. 1a shows the magnetization $M(H)$ curves for ZnO thin films (1) and (2) measured together with sapphire substrate. The $M(H)$ values in Fig. 1a are normalized for the same area of the films and given in emu/cm^2 . In Fig. 1b the central parts (low fields) magnetization curves for the films (1) and (2) are shown without input of sapphire substrate and given in emu/cm^3 . In Fig. 1c the magnetization curve for the film (2) is shown without substrate input, the $M(H)$ values are given in $\mu\text{Bohr}/\text{f.u.}$. The magnetization curves clearly show the pronounced ferromagnetism indicated by the saturation of magnetization (above the applied field ~ 1 T). $M(H)$ is different for two ZnO films synthesized in different conditions: $M_s(1) = 0.1 \text{ emu}/\text{cm}^3$ and $M_s(2) = 0.7 \text{ emu}/\text{cm}^3$. For the film (1) $M_s = 27 \cdot 10^{-6} \text{ emu}/\text{cm}^2$ is very close to the substrate input of about

$24 \cdot 10^{-6} \text{ emu}/\text{cm}^2$. The saturation magnetization of the film (2) corresponds to about $2 \cdot 10^{-3} \mu\text{Bohr}/\text{f.u.}$ It is, therefore, comparable with previously obtained data [6]. The inset shows the central part of the magnetization curve for the sample (2). Both branches of magnetization curve are very close to each other at zero field. However, the coercivity is about 0.01 T at the applied field of 0.2–0.4 T. Thus, similar to our previous work [6] we observe a clear saturable ferromagnetic like RT behavior in the pure, undoped ZnO without any magnetic impurity.

Fig. 2a shows the bright field high-resolution TEM micrograph of ZnO film (1) annealed in argon at 650°C for 0.5 h. This sample possesses very weak FM with $M_s(1) = 27 \cdot 10^{-6} \text{ emu}/\text{cm}^2$ (Fig. 1a). A clear crystalline ZnO structure is directly observable in the bright field images for each grain, which are separated from each other

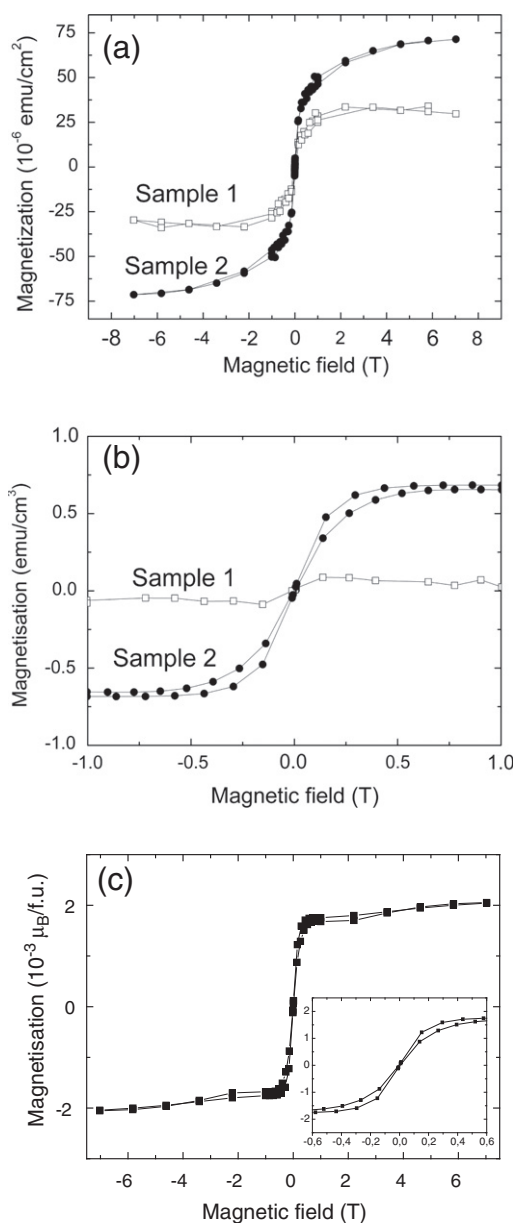


Fig. 1. (a) Magnetization at room temperature for the ZnO thin films 1 (open squares) and 2 (full squares). Magnetization is measured together with sapphire substrate, calibrated in emu/cm^2 . (b) Magnetization for the ZnO thin films 1 and 2 without input of sapphire substrate at low fields, calibrated in emu/cm^3 . (c) Magnetization at room temperature for the ZnO thin film 2, the substrate input is subtracted, the M_s values are given in $\mu\text{Bohr}/\text{f.u.}$. The inset shows the central part of the magnetization curve.

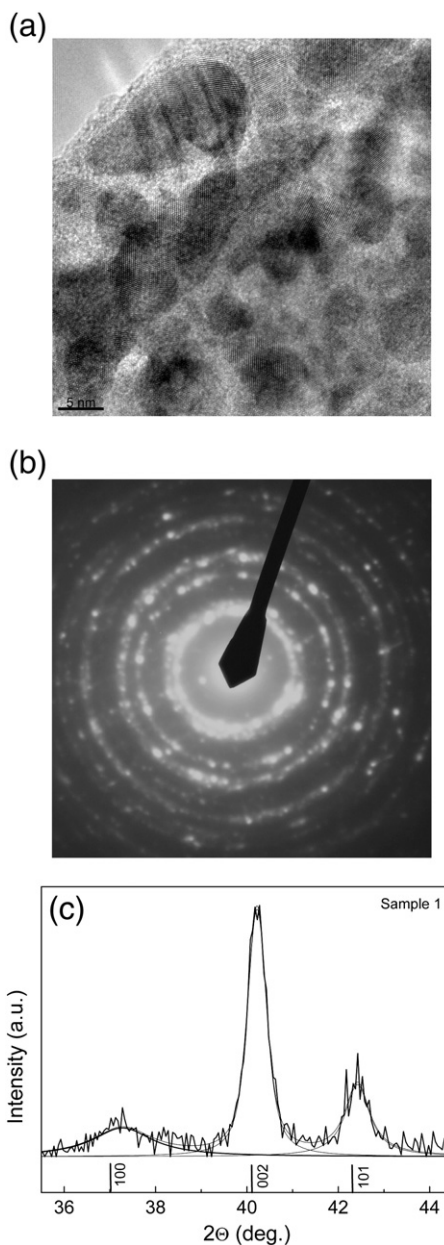


Fig. 2. (a) Bright field high-resolution TEM micrograph of the ZnO film (1) annealed in argon at 650°C , 0.5 h. Crystalline ZnO grains with wurtzite structure are separated from each other by thin amorphous layers. (b) The respective selected area electron diffraction (SAED) pattern. The positions of wurtzite reflections and weak amorphous halo are shown. (c) X-rays diffraction spectrum. The background is subtracted and the spectrum is deconvoluted (three thin lines). It consists of three wurtzite peaks 110, 002 and 101. The halo from the amorphous phase is negligible.

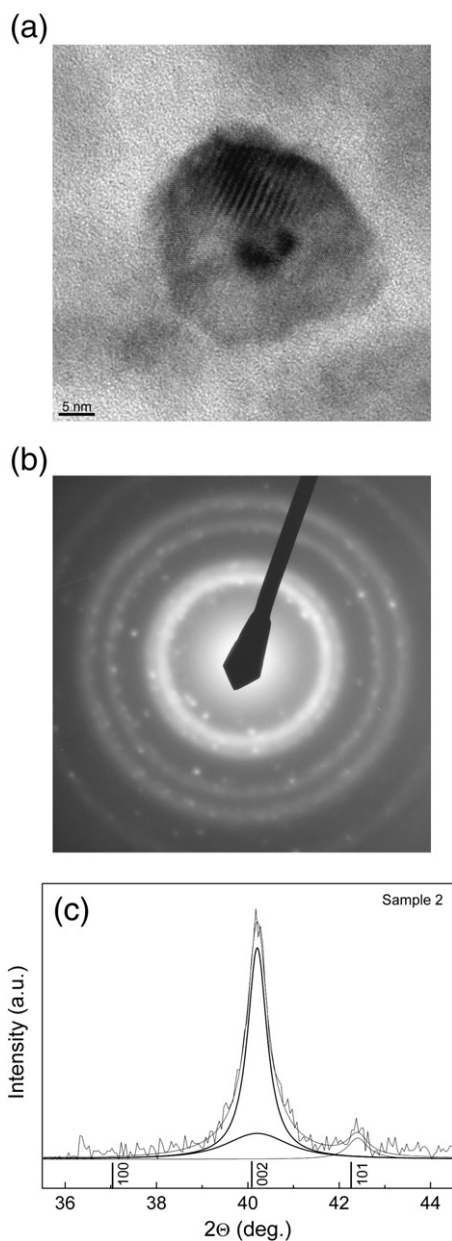


Fig. 3. (a) Bright field high-resolution TEM micrograph of the ZnO film (2) annealed in argon at 550 °C, 24 h. Crystalline ZnO grains with wurtzite structure are surrounded by the amorphous areas. (b) The respective SAED pattern. The positions of wurtzite reflections and strong amorphous halo are shown. (c) X-rays diffraction spectrum. The background is subtracted and the spectrum is deconvoluted (three thin lines). It consists of the halo from the amorphous phase (low peak in the middle) which is superimposed over the 002 peak (high peak in the middle) and 101 peak (low peak right) of crystalline wurtzite ZnO phase. Peak 100 is absent.

by thin (2 to 5 nm) amorphous layers. The respective selected area electron diffraction (SAED) pattern contains the reflections of wurtzite ZnO phase and weak amorphous halo (Fig. 2b). The X-rays diffraction spectrum in Fig. 2c contains three peaks corresponding to the 100, 002 and 101 reflections of the ZnO with hexagonal wurtzite structure. The deconvolution of the XRD spectra into separate peaks was made using the Origin software. The peaks were fitted using the Voigt function. Before the deconvolution the background subtraction procedure had been applied to the spectra. The results of the deconvolution are shown by three thin lines under the experimental X-rays intensity curve. The halo from the amorphous phase is negligible.

Fig. 3a contains the bright field high-resolution TEM micrograph of the ZnO film (2) annealed in argon at 550 °C, 24 h. This film is ferromagnetic with $M_s(2) = 75 \cdot 10^{-6}$ emu/cm² (Fig. 1a) or $2 \cdot 10^{-3}$ μ Bohr/f.u. (Fig. 1b). Crystalline ZnO grains with wurtzite structure are surrounded by the broad amorphous areas. The SAED pattern (Fig. 3b) contains the wurtzite reflections and strong amorphous halo. The X-rays diffraction spectrum (Fig. 3c) consists of the halo from the amorphous phase (low peak in the middle) which is superimposed over the 002 and 101 peaks of crystalline wurtzite ZnO phase. The 101 peak is weak in comparison with that in the sample (1), Fig. 2c. The peak 100 is completely absent. It means that the grains in sample (1) are oriented randomly and sample (2) is textured. Comparing the integral intensities of two crystalline peaks and of the amorphous halo in Fig. 3c allows a rough estimation of the amount of amorphous phase, which is about 15%.

Therefore, the M_s definitely increases with increasing amount of intergranular amorphous phase. In our previous work we demonstrated that the M_s dependence on Mn concentration is different in (nanograined) Mn:ZnO samples manufactured with different methods. For example, M_s drastically changes with changing topology of the GB network in the Mn-doped zinc oxide [9]. Most probably, the ferromagnetism in ZnO is not only driven by the defects. Moreover, the proper combination and topology of interpenetrating crystalline and amorphous phases is needed for the ferromagnetism in pure ZnO.

The defects and non-uniformity of spatial distribution of dopant atoms in ZnO are frequently discussed as a possible reason for the FM behavior [5 and references therein]. However, even without dopants ZnO remain a two-component system. And it is known that in the two- and multicomponent systems the composition of intergranular layers differs from the bulk composition [13,14]. This difference is even more pronounced in case if the GBs are thicker than one atomic monolayer [15]. In other words, the observed amorphous regions separating the crystalline grains with wurtzite structure can be oxygen-deficient. These interconnected amorphous layers form the “ferromagnetic GB foam” in zinc oxide.

4. Conclusions

Thus, we can conclude that (1) ferromagnetic behavior can be observed in pure ZnO even without magnetic dopants, (2) the presence of a dense grain boundary network is a necessary but not sufficient condition for the ferromagnetism in pure ZnO, (3) the microstructure of intergranular layers in ZnO can be tailored by adjusting the synthesis conditions, (4) saturation magnetization M_s depends on the structure of intergranular layers in ZnO, (5) M_s increases with increasing amount of intergranular amorphous phase, (6) most probably the proper combination of interpenetrating crystalline and amorphous phases is the condition for the ferromagnetism in pure ZnO.

Acknowledgments

Authors thank the Russian Foundation for Basic Research (grants 11-02-92694, 11-08-90439, 11-03-00029 and 10-02-00086) for the financial support.

References

- [1] Singhal RK, Kumar S, Xing YT, Deshpande UP, Shripathi T, Dolia SN, Saitovitch E. Mater Lett 2011;65:1485–7.
- [2] Sebastian KC, Chawda M, Jonny L, Bodas D. Mater Lett 2010;64:2269–72.
- [3] Singhal RK, Samariya A, Kumar S, Xing YT, Saitovitch E. Mater Lett 2010;64:1846–9.
- [4] Dietl T, Ohno H, Matsukura F, Cibert J, Ferrand D. Science 2000;287:1019–22.
- [5] Dietl T. Nat Mater 2010;9:965–74.
- [6] Straumal BB, Mazilkin AA, Protasova SG, Myatiev AA, Straumal PB, Schütz G, van Aken PA, Goering E, Baretzky B. Phys Rev B 2009;79:205206.
- [7] Hong NH, Sakai J, Brizé V. J Phys Cond Mat 2007;19:036219.

- [8] Hu YM, Wang CY, Lee SS, Han TC, Chou WY. *Thin Solid Films* 2010;519:1272–6.
- [9] Straumal BB, Protasova SG, Mazilkin AA, Myatiev AA, Straumal PB, Schütz G, Goering E, Baretzky B. *J Appl Phys* 2010;108:073923.
- [10] Straumal BB, Myatiev AA, Straumal PB, Mazilkin AA, Protasova SG, Goering E, Baretzky B. *JETP Lett* 2010;92:396–400.
- [11] Straumal BB, Mazilkin AA, Protasova SG, Myatiev AA, Straumal PB, Baretzky B. *Acta Mater* 2008;56:6246–56.
- [12] Chiu WS, Khiew PS, Isa D, Cloke M, Radiman S, Abd-Shukor R, Abdullah MH, Huang NM. *Chem Eng J* 2008;142:337–43.
- [13] Divinski SV, Lohmann M, Herzig Chr, Straumal B, Baretzky B, Gust W. *Phys Rev B* 2005;71:104104.
- [14] Straumal BB, Mazilkin AA, Kogtenkova OA, Protasova SG, Baretzky B. *Phil Mag Lett* 2007;87:423–30.
- [15] Luo J. *Crit Rev Sol State Mater Sci* 2007;32:67–109.